Journal of Cluster Science (2018) 29:177–184
https://doi.org/10.1007/s10876-017-1317-7

ORIGINAL PAPER

Gold-Carboxymethyl Cellulose Nanocomposites Greenly Synthesized for Fluorescent Sensitive Detection of Hg(II)

Gang Li[1,2] · Yonglin Sun[1] · Huihong Liu[2]

Received: 27 July 2017 / Published online: 9 December 2017

Abstract
The green synthesis of gold nanoparticles, using carboxymethyl cellulose as both capping agents and reducing agents, is an environmental friendly, simple and efficient route for synthesis of metallic nanoparticles. The optimal conditions, such as the ratio of 0.5 mM $HAuCl_4$ against 0.4% CMC; temperature 80 °C; solution pH 9.0 and reaction duration 50 min, were established to produce the narrower distribution, the smaller and more stable AuNPs-CMC. The spherical gold nanoparticles-carboxymethyl cellulose nanocomposites (AuNPs-CMC) with an average particle size of 20.3 ± 5.5 nm was confirmed by the techniques such as high transmission electron microscopy, energy dispersive X-ray spectroscopy, selected area electron diffraction pattern and dynamic light scattering. The as-synthesized AuNPs-CMC with a SPR absorption band of 522 nm can be used as fluorescent probes for the detection of Hg(II) in the range of 0.05–0.32 μM with a detection limit of 3.6 nM. This study essentially paves the way for the generation of functional materials with coupled optical properties and as an analytical platform for rapid and selective detection of metal ions.

Keywords Carboxymethyl cellulose · Gold nanoparticles · Green synthesis · Fluorescence · Mercury ion

Introduction

With nanotechnology, a large set of materials and improved products rely on a change in the physical properties when the feature sizes are shrunk. These nanomaterials are used in many applications such as sensors, water purification, antimicrobial, catalysis, biomedical, agricultural etc. [1, 2]. Gold nanoparticles (AuNPs) display interesting catalytic, optical, electrical, magnetic and chemical properties due to quantum–mechanical rules [3]. The broad range of applications of AuNPs can be attributed to these properties, which are tunable with their size, stabilizing or capping agents [4]. Various methods have been developed for the preparation of AuNPs for the special application [5]. Gold nanoparticles are typically obtained by chemical reduction of tetrachloroauric acid. However this conventional approach is based on the use of external chemical reductants that often produce undesired side products. Therefore a series of green methods have recently been developed to prepare AuNPs with good water solubility, low toxicity, biocompatibility and surface functionalization [6]. Among all reported reducing/capping agents, polysaccharides were seen as a possible eco-friendly approach for the synthesis of Au-NPs [7, 8]. The superiority of polysaccharides, compared with other agents, relies on the fact that these materials are sustainability in nature and non-toxic biocompatibility. Additionally, there are several other interesting benefits such as the ability to form a shell around the gold nanoparticles for an excellent robustness against agglomeration in various extreme conditions and can self-assemble into nanostructures acting as structure-directing agents during crystal growth [9].

Carboxymethyl cellulose (CMC) is a widely used cellulose derivative due to its non-toxicity, biocompatibility, and biodegradable [10–12]. It has been applied in various industries such as food industry, oil industry, medicine industry, paper industry, textile industry and so on [13, 14].

✉ Yonglin Sun
sunyonglin2011@163.com

✉ Huihong Liu
huihongliu@126.com

[1] College of Chemical Engineering and Food Science, Hubei Liberal and Arts University, Xiangyang 441053, China

[2] Analysis and Measurement Center, Wuhan Textile University, Wuhan 430200, China

Because of its special structure and properties, CMC can be used as a template to guide the growth of nano metal crystals [15–17] (Scheme 1).

Mercury is the well-known highly toxic and widely spread heavy metal pollutant [18, 19]. Mercury exposure at high levels can harm the brain, heart, kidneys, lungs, and immune system of people of all ages [20]. The permissible exposure limit (PEL) of mercury exposure in air determined by the occupational safety and health administration (OSHA, PEL) was 0.05 mg m^{-3} [21]. However mercury has excellent performances and is used in many aspects. Therefore it is necessary to control the concentration of mercury. For this purpose it is essential to develop fast, simple, and highly sensitive methods for detecting Hg(II).

AuNPs have become promising luminescent nanomaterials for detection of Hg(II) due to high selectivity and ultra-sensitivity [22–25]. The colorimetric behavior of AuNPs is related to their plasmon absorption in the visible or near-infrared region. The surface plasmon resonance (SPR) stems from the free electrons at the metal surface collectively resonating with the incident photons. SPR strongly depends on particle size, shape, geometry, refractive index of the medium, inter particle distance and aggregation state in solution [26].

The use of environmentally benign to combine renewable materials and nanoparticles has attracted tremendous attention from both academia and industry. This paper presents an effective route to synthesize AuNPs with eco-friendly CMC in one spot. The roles of CMC in the synthesis of AuNPs are to act as a reducing agent and stabilizing ligand. In order to improve the optical properties of AuNPs-CMC nanocopmsites, the synthesized conditions were easily controlled to modify their size and shape. Herein, we use a green and rapid approach to synthesize the AuNPs which can create a fluorescent sensor providing high sensitivity and selectivity for Hg^{2+} detection.

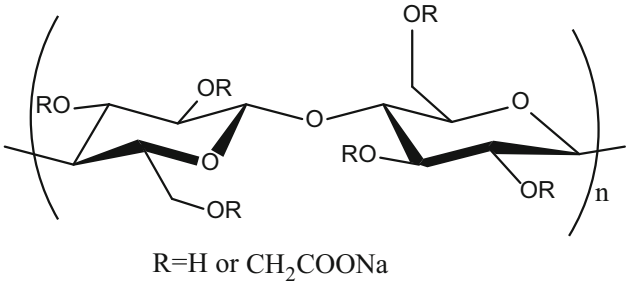

Scheme 1 Structural formula of carboxymethyl cellulose sodium salt

Materials and Methods

Materials

Carboxymethyl cellulose sodium salt (800–1200 cP,) was provided by Shanghai shanpu Chemical Co., Ltd. Chloroauric acid ($HAuCl_4{\cdot}4H_2O$) was purchased from Sinopharm Chemical Reagent Co., Ltd. (Shanghai, China). Other reagents were all of analytical reagent grade. Super-purified water was used throughout all the experiments.

Instrumentation

The UV–visible spectra of Au NPs colloidal solution were measured at room temperature on a UV-8000S spectrophotometer (Shanghai, China). The High resolution transmission electron microscopy (HRTEM) was performed in a JEOL-JEM-2100F equipped with an energy dispersive spectrum (EDS) detector. The XRD pattern of PdNPs was carried out with a Bruker D8 Advance Diffractometer (Bruker AXS, Germany).The reflection absorption-fourier transform infrared (RA-FTIR) spectra of CMC and AuNPs-CMC were obtained using a VERTEX 70 spectrometer (Bruker Corporation, USA). The particle size and distribution and zeta potential were recorded by Malvern ZEN 3600 Zetasizer (England). Fluorescence spectra were recorded by operating the F-2500 spectrophotometer (Hitachi, Japan).

Synthesis of AuNPs

Two grams of CMC was mixed with 200 mL of deionizer water and stirred with a magnetic stirrer at 60 °C for 8 h. The CMC aqueous solution was stored in the refrigerator for further use after cooled at room temperature. For a typical synthesis of AuNPs, an aqueous solution of $HAuCl_4$ (2 mL, 1 mM) was mixed with the varying quantity of CMC solution (1.0, 1.5, 1.8, 2.0, 2.5, 2.8 mL) in a 10 mL flask, and then adjust the reaction mixture solution pH by using NaOH solution. The flask was heated by using a temperature controlled water bath for several minutes.

Fluorescence Measurements

The fluorescence sensing experiments of CMC-AuNPs toward Hg(II) were typically carried out in PBS buffer that was used to adjust the acidity of solution at pH 9.0. Different concentrations of Hg(II) solution were added and mixed thoroughly, and then the mixture was left to equilibrate for 15 min at room temperature before determination. The fluorescence quenching spectra were recorded with excitation at 308 nm.

Results and Discussion

The Synthesis of AuNPs-CMC Nanocomposites

A pale pink color was appeared after mixing the colorless CMC and yellow $HAuCl_4$ for 5 min and the color was gradually intensified as the reaction was continued with heating, indicating the formation of AuNPs (Fig. 1 insert). UV–vis spectroscopy is most commonly used techniques to confirm the formation and stability of metal nanoparticles in aqueous solution. Figure 1a shows the UV–vis spectrum of CMC without any peaks in the region of 250–750 nm. The spectrum (Fig. 1b) shows a single absorption peak at 304 nm, which is attributed to the d–d transition of Au(III) ions [23]. A typical plasmon resonance band appears at 522 nm belong to the formation of AuNPs (Fig. 1c) [23].

AuNPs exhibit striking optical properties due to surface plasmon vibration of conduction electrons depending upon the shape and size of the particles. It was reported that the spherical AuNPs of 13 and 56 nm diameter exhibit large SPR-extinction bands centered at wavelengths of 520 and 530 nm respectively [24]. The different reaction parameters such as concentration of gold salt and CMC, pH, contact time and temperature should be explored to produce stable AuNPs with homogeneous size and morphologies [27].

The optical properties of AuNPs relAu(IIIies on the mass ratio of the metal salt toward the reducing agent in the reaction solution. AuNPs were synthesized by reducing Au(III) to Au(0) at a constant concentration of 0.5 mM $HAuCl_4$ while increasing CMC concentration from 0.2 to 0.6% (w/v) (Fig. 2a). The absorption intensity gradually increased with increasing CMC concentration from 0.2 to 0.4% indicating the formation of greater number of AuNPs. Furthermore the SPR band blue-shifted from 530 to 522 nm implying the decrease of the synthesized particle size. Moreover the absorption peak width gradually becomes narrower suggesting the narrower size distribution of AuNPs [28]. However the absorption intensity decreases a little with increasing CMC concentration further to 0.5 and 0.6%. The optimal CMC concentration in the reaction medium was 0.4%.

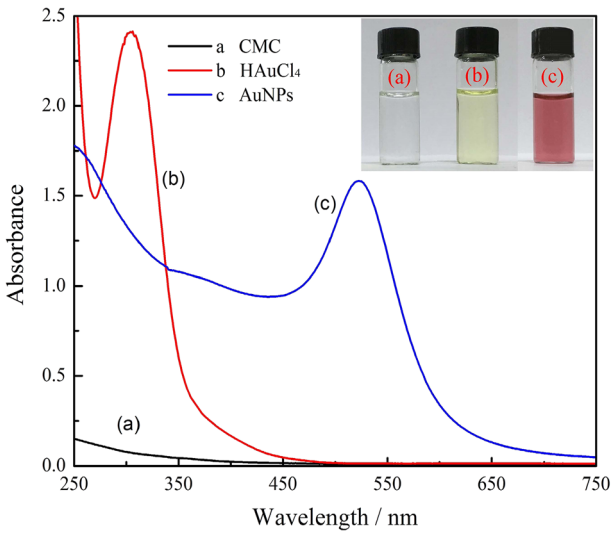

Fig. 1 UV-Vis spectra of **a** CMC aqueous solution, **b** $HAuCl_4$ and **c** as-synthesized AuNPs

It is obvious from the earlier result that higher temperature facilitates the formation of AuNPs of various shapes and size. Figure 2b shows the UV–Vis spectra of AuNPs were prepared at different temperature of 60, 70, 80 and 90. It is as expectation that the absorption intensity increased and a blue shift of the SPR band when the temperature increased from 60 to 80 °C, confirming the positive correlation between the yield of the nanoparticles and the temperature. There is no change in SPR band when temperature is further higher. Thus the temperature of 80 °C was chosen for the following experiments.

An optimum duration is required for complete nucleation and subsequent stability of as-synthesized AuNPs. Figure 2c showed the UV–visible spectra of AuNPs synthesized at different reaction duration. It is observed that the absorption intensity was increased and SPR band was shifted blue with the reaction duration increasing from 30 to 50 min. The maximum intensity of absorption with a typical SPR band at 522 nm was appeared after the reaction has been taken for 50 min. So the reaction duration was determined as 50 min.

It is evidential that the pH of the reaction solution may play a decisive role in the synthesis of AuNPs [29]. Figure 2d shows the UV–Vis spectra of colloidal gold solution formed at pH 7.0, 8.0, 9.0, 10.0, 11.0 and 12.0. It was observed that there was an increase in absorption and a blue-shift in peak from pH 7.0 to pH 9.0, indicating higher pH facilitates the nucleation and subsequent formation of a large number of nanoparticles with smaller diameter [30]. However a decrease in absorption and a red-shift in peak from pH 10.0 to pH 12.0 were obtained. Thus the reaction solutions were adjusted to pH 9.0 for the synthesis.

The Characterization of AuNPs-CMC Nanocomposites

In the present research account, the narrower distribution, the smaller and more stable AuNPs were synthesized at the optimal conditions as the following: the ratio of 0.4% CMC against 0.5 mM $HAuCl_4$; temperature 80 °C; solution pH 9.0 and reaction duration 50 min.

The particle size distribution of as-synthesized AuNPs was determined by using dynamic light scattering (DLS) principle and presented in Fig. 3. The dispersity of AuNPs

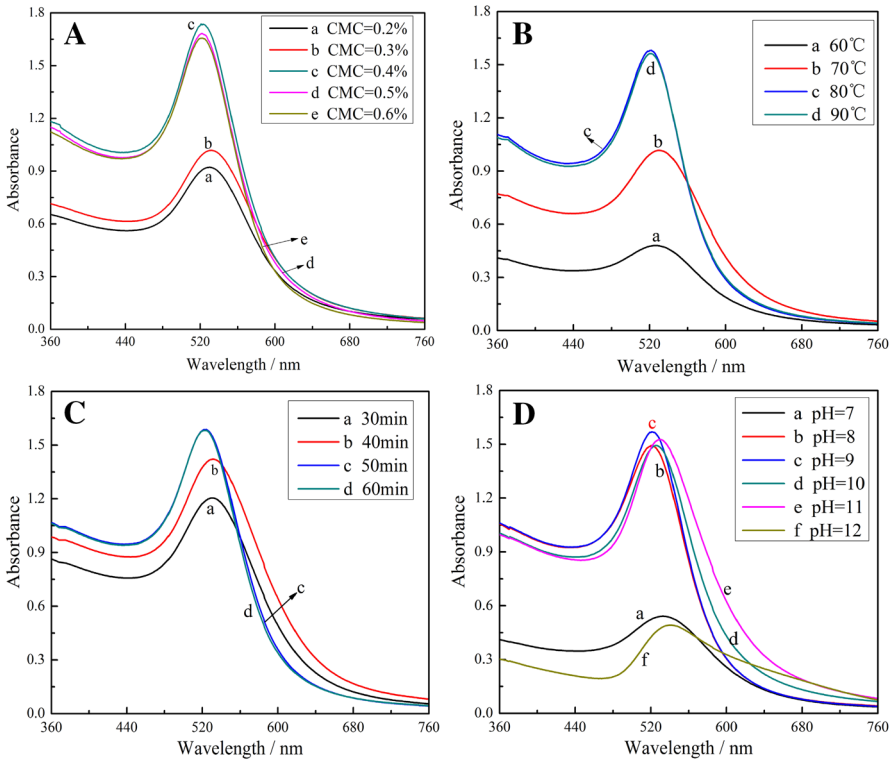

Fig. 2 UV–Vis spectra of AuNPs formed at different concentrations of CMC (**a**), temperatures (**b**), durations (**c**) and pHs (**d**)

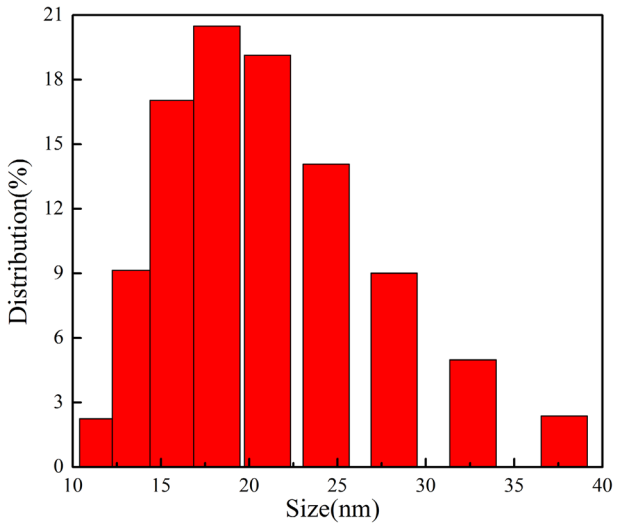

Fig. 3 Size distributions of AuNPs

is 13.5–28.2 nm (cover the 90% of the all nanoparticles) with an average particle size of 20.3 ± 5.5 nm was estimated. Additionally the SPR absorption band was around 522 nm that is coincided with the results of earlier report [23].

The shape, morphology and elements of the as-synthesized AuNPs were analyzed using the high resolution transmission electron microscopy (HRTEM) equipped with an energy dispersive X-ray spectroscopy (EDX). HR-TEM image (Fig. 4a) showed that the particles are mostly spherical with a few having rod and decahedral morphology. The average particle size of 19.8 nm estimated from the typical HRTEM images is little smaller than that measured using dynamic light scattering (DLS). The typical high-resolution TEM image (Fig. 4b) with clear lattice fringes having a spacing of 0.231 and 0.204 nm reveals that the growth of AuNPs occurs preferentially on the (111) and (200) planes in face-centered cubic gold crystal, respectively [30]. The selected area electron diffraction (SAED) pattern (Fig. 4c) shows the different rings indexing as (111), (200), (220) and (311) Bragg reflections which further confirmed the crystalline AuNPs as face centered cubic structure [31]. Clear lattice fringes in high resolution TEM image and the typical SAED pattern with bright circular rings show that the nanoparticles are highly crystalline. EDX spectrum shows the clear signals for gold located at 2.2 and 9.8 keV (Fig. 4d).

XRD patterns of AuNPs-CMC (Fig. 5) shows the presence of all the characteristic diffraction peaks of face centered cubic (fcc) gold belonging to (111), (200) and (220) diffraction lines at $2\theta = 38.4°$, 44.3° and 64.8°, respectively (JCPDS No. 99-0056). The majority of particles showing (1 1 1) plane having fcc structure.

RA-FTIR measurements have also been conducted to show the existence of the CMC molecules on the surface of the AuNPs (Fig. 6). For pure CMC (Fig. 6a), the broad transmission bands at 2842–3037 cm^{-1} with a maximum at 2935 cm^{-1}, is attributed to the asymmetric and symmetric

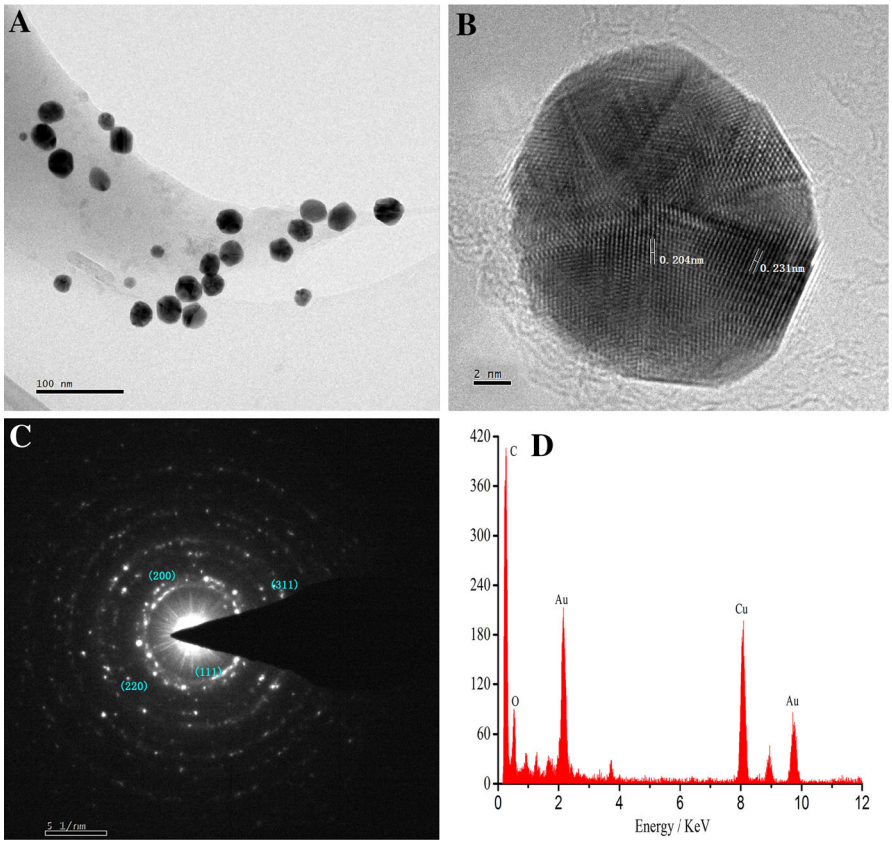

Fig. 4 TEM image of AuNPs (**a**) and HRTEM imagewith spacing of lattice fringes selected-area (**b**), electron diffraction (SAED) pattern (**c**) and EDX spectrum (**d**)

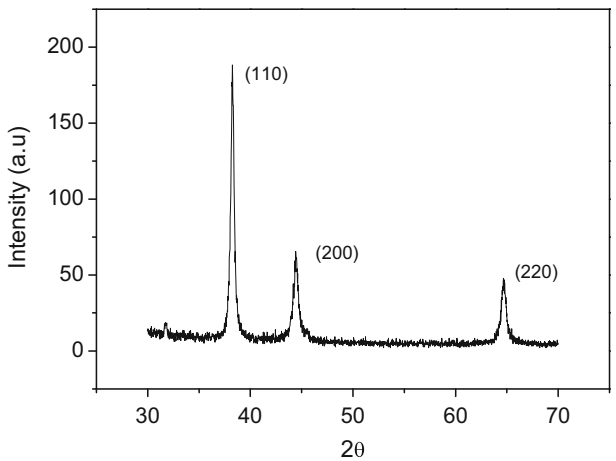

Fig. 5 XRD pattern of AuNPs-CMC

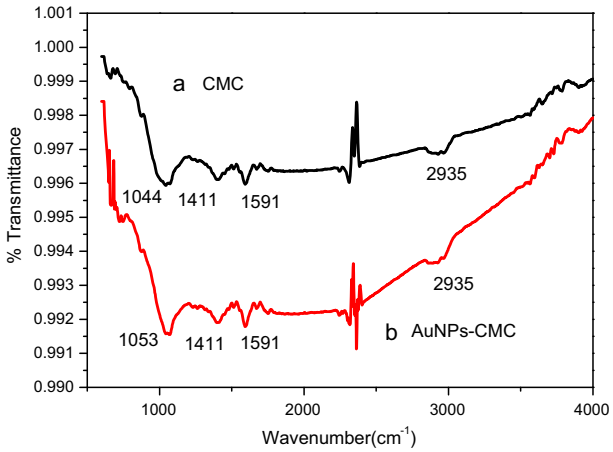

Fig. 6 RA-FTIR spectra, **a** pure CMC and **b** AuNPs-CMC

CH2 stretching. The absorption bands observed at 1591 $cm^{-1}$is characteristic of propyl stretching vibrations. The peak at 1411 cm^{-1} is assigned to the C–H bending vibration. The asymmetric C–O–C stretching vibrations of cyclic ethers and the C–O stretching vibrations in C–OH are observed at 1044 cm^{-1}. Compared with Fig. 6a, the peak at 1044 cm^{-1} is shifted to 1053 cm^{-1} in the spectrum of the AuNPs coated with CMC (Fig. 6b). These differences indicated that a chemical bond between the gold atom and oxygen atom of CMC has been formed. By this way, the CMC molecules are strongly adsorbed on the surface of AuNPs.

It was found that the AuNPs colloidal suspension could remain stable more than one year. Zeta potential values reveal information regarding the surface charge and stability of nanoparticles [32]. The zeta potential value of the as-synthesized AuNPs was measured to be − 37.1 mV (Fig. 7), indicating the negative charges from the carbonyl and hydroxyl groups of CMC form a coat over the AuNPs

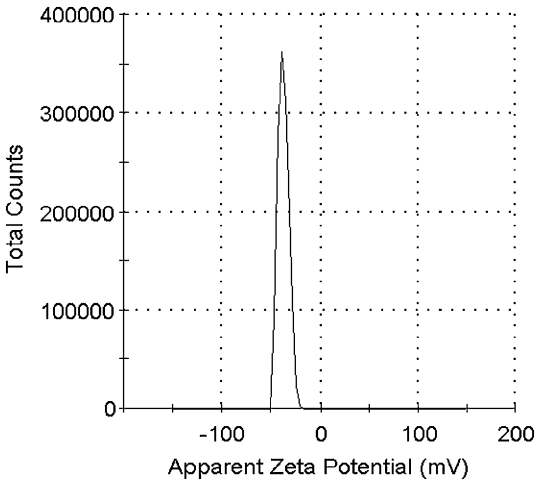

Fig. 7 Zeta potential of the AuNPs solution

and the electrostatic repulsion to prevent aggregation of particles in the colloidal solution.

Optimization of the Fluorescent Sensing Hg(II) by AuNPs-CMC

The fluorescent water-soluble AuNPs-CMC was obtained through green, "one-pot" synthetic route as mentioned above. It is worth to note that reaction temperature, reaction time and the concentration of gold source and reducing

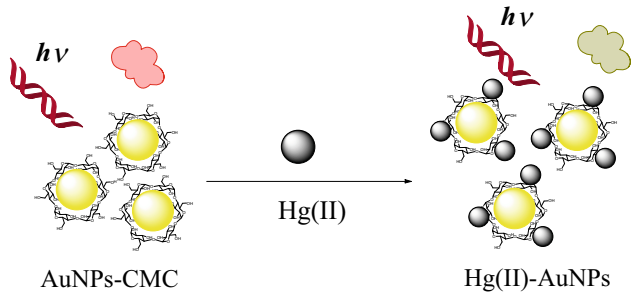

Scheme 2 Schematic illustration of the fluorescent sensing of Hg(II) with AuNPs-CMC composites

agents play important roles in size and yields of AuNPs. The maximum fluorescence emission wavelength of the AuNPs-CMC was centered at 416 nm upon excitation at 308 nm (Fig. 8a).

The effect of pH on the relative fluorescence intensity (ΔF) of AuNPs-CMC was investigated in the pH range from 3.0 to 12.0 for Hg(II) sensing (Fig. 8b). It was found that the fluorescence intensity of the AuNPs-CMC reacting with Hg(II) slightly influenced from pH 5.0 to pH 11.0. Considering the synthesis of AuNPs-CMC at pH9.0, pH 9.0 may be used consequently for the reaction between Hg(II) and the AuNPs-CMC in the experiments.

The selectivity of AuNPs-CMC for fluorescent sensing heavy metals was investigated. Here nine heavy metals such as Hg(II), Bi(III), Pb(II), Cu (II), As (III), Co (II), Ni

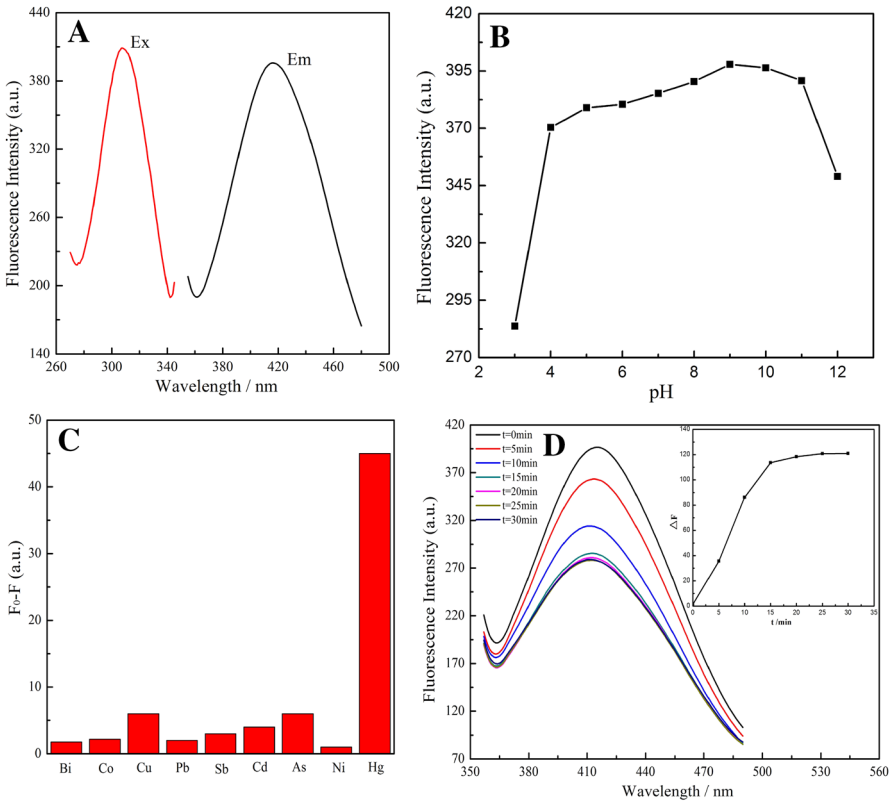

Fig. 8 Fluorescence spectra of AuNPs (**a**), the fluorescence intensities of Au NPs against pH values (**b**), fluorescence intensity histograms of Au NPs in the presence of different metal ions (**c**), and the fluorescence intensities of Au NPs against reaction time (**d**)

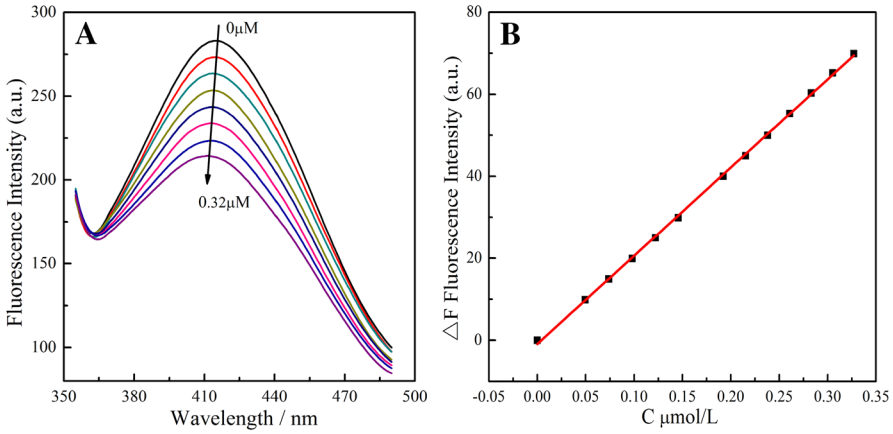

Fig. 9 Fluorescence spectra of AuNPs by adding Hg(II) concentrations (**a**), the fluorescence intensity plotted against the Hg(II) concentration (**b**)

Table 1 Comparison of different fluorescent probes for the determination of Hg(II)

Reagents	Linear range	LOD (nM)	Method
Au NPs-MPA + RB	1.5–2.5 μM	10	[33]
PBA-Au NPs/P(NIPAM–co–DMA)	0.16–1.6 μM	31	[34]
H_2O_2–Amplex UltraRed–Au NP	5–1000 nM	4	[35]
Au NPs–MSD	0.02–1.0 μM	16	[36]
OliGreen-DNA-Au NPs	0.05–2.5 μM	25	[37]
Cytidine-AuAg NCs	0.03–16 μM	30	[38]
Au NPs-DNA	20–90 nM	8	[39]
CMC-AuNPs	0.05–0.32 μM	3.6	This work

MPA Mercaptopropionic acid, *RB* Rhodamine B, *P(NIPAM–co–DMA)* Poly (N-isopropylacrylamide-co-2-(dimethylamino) ethylmethacrylate), *PBA* pyrenebutyric acid, *MSD* mercury specific-aptamer DNA

(II), Cr(VI) and Sb (III) were examined. These heavy metals are forbidden to use in eco-textile products. It was found that the fluorescence of the AuNPs-CMC was efficiently quenched by Hg(II) better than other metal ions (Fig. 8c). Previous literature reports have shown that there are high-affinity metallophilic interactions between the Hg(II) d^{10} and Au(I) d^{10} [4]. The schematic illustration of the fluorescent sensing of Hg(II) with AuNPs-CMC composites is as shown the following Scheme 2.

The effect of incubation time on the relative fluorescence intensity of the system is displayed in Fig. 8d. The fluorescence intensity of AuNPs-CMC decreases in the presence of Hg(II) especially in the 15 min. period and further increase in the incubation time does not cause any drop in the intensity, indicating that the reaction between Hg(II) and AuNPs has reached a state of equilibrium. As such, incubation for 15 min at room temperature was chosen for the subsequent experiments.

Sensitivity of the Fluorescent Sensing Hg(II)

Under the optimal conditions, the capability of the proposed sensor for quantitative detection of Hg(II) was evaluated. As shown in Fig. 9a, the AuNPs-CMC system shows strong fluorescence in the absence of Hg(II). Upon addition of Hg(II) to the solution of AuNPs-CMC, the fluorescence intensity decreased obviously. The Fig. 9b shows the response of the sensor which is fitted with the Stern–Volmer model. A linear correlation between the relative fluorescence intensity (ΔF) and the concentration of Hg(II) over the range of 0.05–0.32 M with a correlated coefficient of $R^2 = 0.9996$ is found. The limit of detection (LOD) for Hg(II) estimated to be 3.6 nM.

In comparison with other fluorescence methods as shown in Table 1, these analytical parameters are comparable or even better than those reported in the literature.

Conclusion

In summary, the stable AuNPs have been synthesized using CMC solution without other reducing agents. It uses a simple metal salt and a reducing agent/template from renewable raw materials. The only side products of the reaction are oxidized cellulose fragments and reduction products from the gold salt. AuNPs-CMC can serve as an effective fluorescent sensing probe for sensitive and selective detection of Hg(II).

Acknowledgements The authors thank the Foundation for Fostering Talents (2016zk017), Discipline Groups Project for Food Industrialization (2017xk008) from Hubei University of Arts and Sciences, and Discipline Innovation Team Project from Wuhan Textile University (201320) for the kind support of this work.

References

1. S. Pandey (2017). *J. Mol. Liq.* **241**, 1091–1113.
2. S. Pandey and S. B. Mishra (2014). *Carbohydr. Polym.* **113**, 525–531.
3. M. Cui, Y. Zhao, and Q. Song (2014). *Trend Anal. Chem.* **57**, 73–82.
4. R. Jin, C. Zeng, M. Zhou, and Y. Chen (2016). *Chem. Rev.* **116**, 10346–10413.
5. F. Dumur, A. Guerlin, E. Dumas, D. Bertin, D. Gigmes, and C. R. Mayer (2011). *Gold Bull.* **44**, 119–137.
6. Y. Park, Y. N. Hong, A. Weyers, Y. S. Kim, and R. J. Linhardt (2011). *Iet Nanobiotechnol.* **5**, 69–78.
7. B. R. Gangapuram, R. Bandi, R. Dadigala, G. M. Kotu, and V. Guttena (2017). *J. Clust Sci.*. https://doi.org/10.1007/s10876-017-1264-3.
8. S. Pandey and K. K. Nanda (2016). *ACS Sens.* **2016**, (1), 55–62.
9. A. Banerjee, U. Halder, and R. Bandopadhyay (2017). *J. Clust Sci.* **28**, 1803–1813.
10. A. Sannino, C. Demitri, and M. Madaghiele (2009). *Materials* **2**, 353–373.
11. D. D. Britto and O. B. G. Assis (2009). *Thermochim. Acta* **494**, 115–122.
12. X. Y. Wang and J. F. Su (2014). *Mater. Sci. Technol.* **30**, 534–539.
13. X. Yang and W. Zhu (2007). *Cellulose* **14**, 409–417.
14. M. J. Waring and D. Parsons (2001). *Biomat.* **22**, 903–912.
15. C. R. Wang, X. Z. Yan, L. L. Yu, and H. Zhou in J. M. Zeng, Y. H. Kim, and Y. F. Chen (eds.), *New Materials, Applications and Processes, Pts 1–3*, vol. 399–401, 2012, pp. 585–588.
16. R. R. Bhattacharjee, M. H. Rashid, and T. K. Mandal (2008). *J. Nanosci. Nanotech.* **8**, 3610–3615.
17. M. N. Nadagouda and R. S. Varma (2007). *Biomacromol.* **8**, 2762–2767.
18. D. W. Boening (2000). *Chemosphere* **40**, 1335–1351.
19. Y. Wang, F. Yang, and X. Yang (2010). *ACS Appl. Mater. Interfaces* **2**, 339–342.
20. USEPA, Environmental protection agency. In: *Mercury*. (2015). http://www.epa.gov/mercury/effects.htm#meth.
21. OSHA, *Occupational Safety & Health Administration: Annotated OSHA Z-2 Table (WWW Document)* (2016). https://www.osha.gov/dsg/annotated-pels/tablez-2.html.
22. E. M. Nolan and S. J. Lippard (2008). *Chem. Rev.* **108**, 3443–3480.
23. Y. H. Lin and W. L. Tseng (2010). *Anal. Chem.* **82**, 9194–9200.
24. W. Chansuvarn, T. Tuntulani, and A. Imyim (2015). *Trac-Trend Anal. Chem.* **65**, 83–96.
25. D. Ghosh and N. Chattopadhyay (2015). *J. Lumin.* **160**, 223–232.
26. Y. Xia and N. J. Halas (2005). *MRS Bull.* **30**, 338–348.
27. Y. Li, G. Li, W. Li, F. Yang, and H. H. Liu (2015). *Nano* **10**, 1.
28. J. L. Gardea-Torresdey, K. J. Tiemann, G. Gamez, and K. Dokken (1999). *J. Nano Res.* **1**, 397–404.
29. V. Armendariz, I. Herrera, J. Peralta-Videa, M. Jose-Yacaman, H. Troiani, P. Santiago, and J. L. Gardea-Torresdey (2004). *J. Nano Res.* **6**, 377–382.
30. S. Pandey, G. K. Goswami, and K. K. Nanda (2013). *Carbohydr. Polym.* **94**, 229–234.
31. M. X. Guo, W. Li, F. Yang, and H. H. Liu (2015). *Spectrochim. Acta A Mol. Biomol. Spectrosc.* **142**, 73–79.
32. Y. Zhang, M. Yan, J. Jiang, P. Gao, G. Zhang, M. M. F. Choi, C. Dong, and S. Shuang (2016). *Sens. Actuators B Chem.* **235**, 386–393.
33. C. C. Huang and H. T. Chang (2006). *Anal. Chem.* **78**, 8332–8338.
34. Y. Tang, Y. Ding, T. Wu, L. Lv, and Z. Yan (2016). *Sens. Actuators B Chem.* **228**, 767–773.
35. C. I. Wang, C. C. Huang, Y.-W. Lin, W.-T. Chen, and H.-T. Chang (2012). *Anal. Chim. Acta* **745**, 124–130.
36. D. Tan, Y. He, X. Xing, Y. Zhao, H. Tang, and D. Pang (2013). *Talanta* **113**, 26–30.
37. C. W. Liu, C.-C. Huang, and H.-T. Chang (2008). *Langmuir* **24**, 8346–8350.
38. Y. Zhang, H. Jiang, and X. Wang (2015). *Anal. Chim. Acta* **870**, 1–7.
39. G. Wang, Y. Lu, C. Yan, and Y. Lu (2015). *Sens. Actuators B Chem.* **211**, 1–6.